

# Efficient Point Clouds Upsampling via Flow Matching

Zhi-Song Liu<sup>1</sup>, Chenheng He<sup>2\*</sup>, Lei Li<sup>3</sup>

<sup>1</sup>Lappeenranta-Lahti University of Technology LUT

<sup>2</sup>The Hong Kong Polytechnic University

<sup>3</sup>Technical University of Munich

zhisong.liu@lut.fi, chenheng.he@polyu.edu.hk, lilei.cg@gmail.com

## Abstract

Diffusion models are a powerful framework for tackling ill-posed problems, with recent advancements extending their use to point cloud upsampling. Despite their potential, existing diffusion models struggle with inefficiencies as they map Gaussian noise to real point clouds, overlooking the geometric information inherent in sparse point clouds. To address these inefficiencies, we propose PUFM, a flow matching approach to directly map sparse point clouds to their high-fidelity dense counterparts. Our method first employs midpoint interpolation to sparse point clouds, resolving the density mismatch between sparse and dense point clouds. Since point clouds are unordered representations, we introduce a pre-alignment method based on Earth Mover’s Distance (EMD) optimization to ensure coherent interpolation between sparse and dense point clouds, which enables a more stable learning path in flow matching. Experiments on synthetic datasets demonstrate that our method delivers superior upsampling quality but with fewer sampling steps. Further experiments on ScanNet and KITTI also show that our approach generalizes well on RGB-D point clouds and LiDAR point clouds, making it more practical for real-world applications.

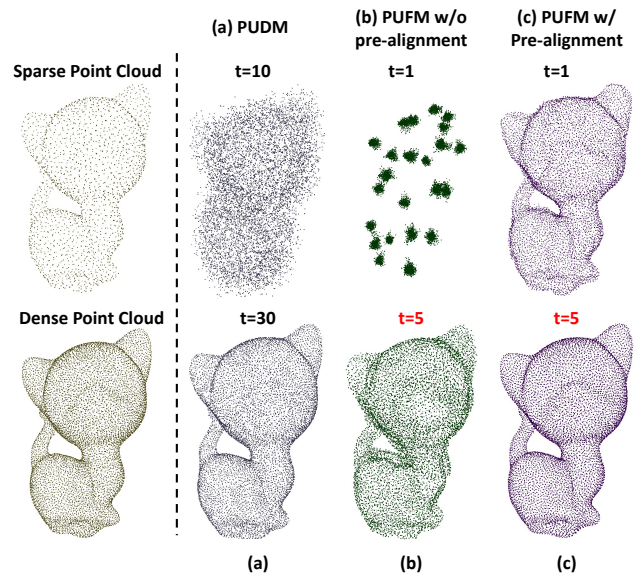


Figure 1: **Convergence comparison among different distribution mapping paths.** The diffusion model PUDM demonstrates slow convergence since it starts from noise distribution. Our proposed PUFM learns flow matching from sparse to dense point clouds. Pre-alignment is applied to minimize the learning ambiguity at the early stage, resulting in a more efficient upsampling process.

## 1 Introduction

Point Cloud Upsampling [Yu and et al., 2018] has been investigated in recent years as a solution to increase the resolution of the point cloud and enhance the geometric details. Higher-resolution point clouds can substantially benefit a range of downstream tasks, including mesh reconstruction [Hanocka and et al., 2020], 3D scene perception [Yang and et al., 2024; Lemke and et al., 2024] and rendering [Kerbl and et al., 2023].

As a fundamentally ill-posed problem, point cloud upsampling has traditionally been approached through conventional methods [Singh and et al., 2007; L. and et al., 2007], which

often rely on computationally expensive optimization techniques and additional priors, such as surface normals or extra point features. However, these methods tend to struggle in more challenging scenarios, particularly when only sparse points are available, making it difficult to infer the underlying topology. Deep learning approaches [Yifan and et al., 2019; He and et al., 2023; Qu and et al., 2024; Li *et al.*, 2019; Rong and et al., 2024] have demonstrated superior performance in point cloud upsampling. By training deep neural networks to encode point cloud geometry into informative deep features, these methods are able to more effectively reconstruct high-resolution point clouds. Among these, PUNet [Yu and et al., 2018] is a pioneering work to learn multi-level features per point and reconstruct the underlying surface based on the contextual information of point set.

Recent advances in diffusion models [Ho and et al., 2020]

\*Corresponding Author

for ill-posed problems have motivated their application to point cloud upsampling. PUDM method [Qu and et al., 2024] proposed a conditional probability diffusion model that treats point cloud upsampling as a noise-to-data generative process, conditioned on the sparse point clouds. This approach has demonstrated high-quality dense prediction for both uniform and nonuniform point clouds. However, we argue that this noise-to-data process is inefficient for point cloud upsampling, as the sparse point clouds themselves already encode the valuable prior information about the target structure. As illustrated in Figure 1a, PUDM exhibits relatively slow convergence in the reconstruction of dense point clouds, suggesting that the reliance on noise generation may be unnecessarily complex for the task at hand.

In this work, we propose **Point cloud Upsampling via Flow Matching (PUFM)**, an efficient method that directly learns the optimal transport between sparse and dense point cloud distributions, significantly reducing both the learning complexity and sampling cost compared to diffusion models. To address the cardinality difference between the two distributions, we first apply midpoint interpolation [He and et al., 2023] to densify the point clouds. However, we observe that the flow matching model encounters ambiguous learning during early stages, as indicated by the collapsed ball-shaped clusters in Figure 1b. This issue arises from the inherent unordered nature of point clouds, which leads to multiple bijective matching paths between the sparse and dense point sets. Due to this inherent ambiguity, the flow matching model tends to learn a suboptimal “average path” during the early steps of training, which slows its convergence. To mitigate this, we propose pre-aligning the sparse point clouds to their corresponding ground-truth by optimizing their Earth Mover’s Distance (EMD). This pre-alignment step helps to reduce the ambiguity in the flow matching process by providing a clearer correspondence between the sparse and dense distributions. The learning trajectory in flow matching becomes much smoother and therefore results in faster convergence during training. Importantly, the pre-alignment is not required during inference. As demonstrated in Figure 1c, the optimized flow matching model is able to reconstruct high-fidelity dense point clouds with only a few sampling steps, achieving both high accuracy and efficiency.

To evaluate the effectiveness of our approach, we apply PUFM to datasets such as PUGAN [Li *et al.*, 2019] and PU1K [Qian and et al., 2021], where it outperforms existing methods, achieving state-of-the-art performance. Furthermore, we extend our method to real-world datasets, including Scannet [Dai *et al.*, 2017] and KITTI [Geiger and et al., 2013]. The qualitative results highlight our method’s ability to reconstruct extremely sparse instances, demonstrating its superior generalization and robustness in diverse scenarios.

## 2 Related Works

### 2.1 Point Clouds Analysis

Different from image data, point clouds contain irregular structures and are invariant to permutation. PointNet [Charles *et al.*, 2017] is the pioneering work that applies shared MLPs to extract point-wise features, and then uses maxpooling

for the extraction of permutation-invariant features. PointNet++ [Qi and et al., 2017] further improves it by proposing set abstraction to extract multi-level features. Similar works can be also found in [Ma and et al., 2022; Qian and et al., 2024; Wang and et al., 2019; Zhang and et al., 2019; Thomas and et al., 2019]. For instance, PVCNN [Lu and et al., 2022] modifies the PointNet++ to handle vocalized point cloud representation, a low rank matrix approximation algorithm is proposed to estimate normals for underlying 3D surface reconstruction. Recently, attention [Vaswani and et al., 2017] has also been widely investigated for point cloud processing. [Guo, 2021; Wu and et al., 2022; Park and et al., 2022; Wu and et al., 2024b; Contributors, 2023; Zhao *et al.*, 2021; Yu and et al., 2021; Wu *et al.*, 2022; Wu and et al., 2024a] have achieved impressive performance for point cloud recognition, denoising and enhancement.

In this work, we build our flow matching model on top of PointNet++ as it encodes multi-level contextual information and produces point-wise representation.

### 2.2 Point Clouds Upsampling

Point cloud upsampling has been extensively studied in recent years, with several approaches proposed to enhance point cloud resolution and improve geometric details. Early learning-based methods, such as PUNet [Yu and et al., 2018], paved the way for using deep learning in point cloud upsampling. MPU [Yifan and et al., 2019] introduced a progressive upsampling technique using patch-based processing, while PUGCN [Qian and et al., 2021] employed graph convolution networks for learning local point information via NodeShuffle. PUBP [Liu and et al., 2023] introduced a back-projection network for iterative down- and up-sampling refinement, and PUGAN [Li *et al.*, 2019] leveraged adversarial networks to supervise the generation distribution, achieving more evenly distributed dense points. Further developments include self-supervised learning methods [Wenbo and et al., 2022; Metzger and et al., 2021] for exploiting local-scale geometric recurrence, as well as methods like PU-Geo [Qian and et al., 2020] and NePs [Feng and et al., 2022] that project point clouds to 2D for continuous upsampling via convolution. Other works [Li *et al.*, 2024; Chen and et al., 2023] focus on combining upsampling and denoising with joint supervision to better integrate point features. Despite these advances, most methods still rely on Chamfer distance, which fails to capture detailed underlying 3D structures in point clouds.

In this paper, we propose a flow matching approach for point cloud upsampling that directly models the transport between sparse and dense point cloud distributions. Unlike previous methods relying on Chamfer distance or displacement-based approaches [Yifan and et al., 2019; Li and et al., 2021; Rong and et al., 2024], our method efficiently learns the mapping between sparse and dense point clouds, which optimize the  $l_2$  loss in an iterative inverse path. Our method is also related to recent work in score-based denoising models [Qu and et al., 2024; Kumbar and et al., 2023] and normalizing flows [Mao *et al.*, 2023], but unlike these approaches, which generate dense point clouds from noise, our method directly generates them from sparse data. By incorporating

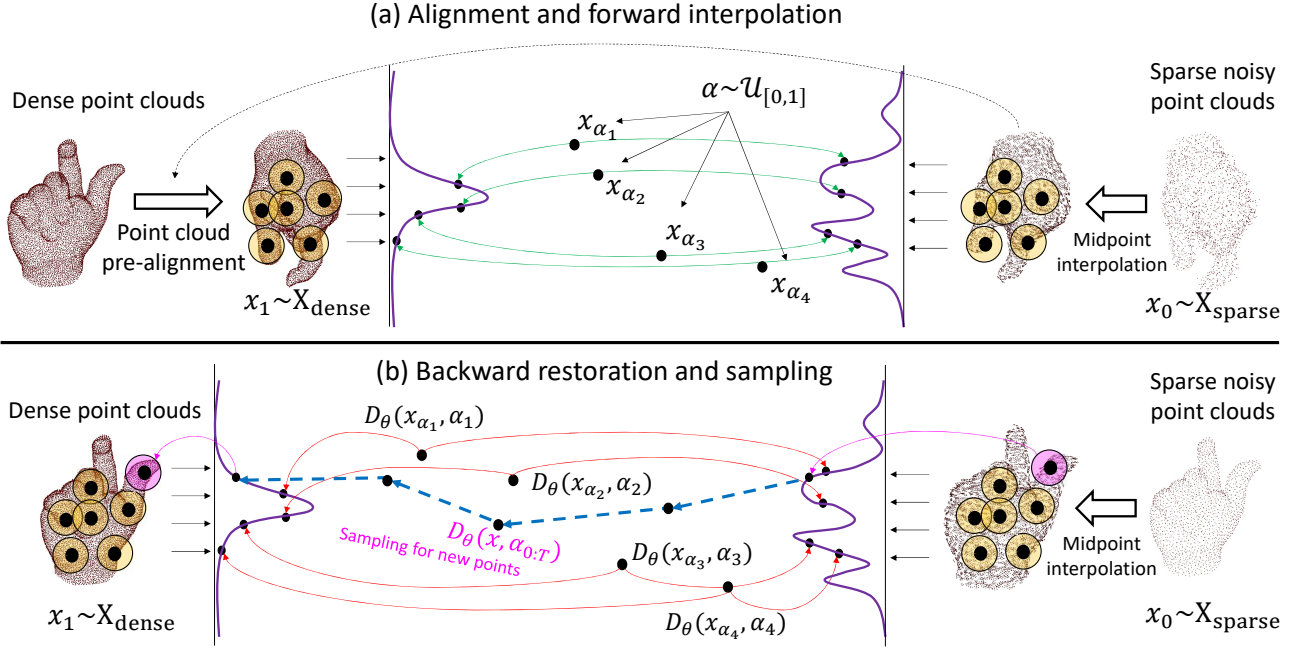


Figure 2: **Illustration of PUFM.** It processes point clouds as patches (yellow circles), and learns  $D_\theta$  to map the distribution from sparse to dense patches. It contains forward alignment and interpolation (a) and backward restoration and sampling (b). In (a), the model first pre-aligns the sparse (initially upsampled by midpoint interpolation) and dense point clouds and then randomly picks “noisy” points as  $x_{\alpha_i}$  with the time step  $\alpha_i$ . In (b), the model optimizes the distribution flow to transform arbitrary sparse data into dense data effectively. During the sampling process, the model directly learns to densify the sparse points without further alignment. Note: the rotated sparse point clouds with 180 degrees illustrate the effect of misalignment between sparse and dense point clouds.

pre-alignment, we significantly reduce permutation ambiguity, enabling faster and more efficient inference.

### 3 Approach

#### 3.1 Preliminary

Given the target data  $x \sim p(x)$ , we aim to build a flow matching generative model [Lipman and et al., 2023] to learn the reverse time-dependent process to obtain noise  $\epsilon \sim N(0, I)$  as,

$$x_t = \alpha_t x + \sigma_t \epsilon, \text{ where } t \in [0, 1] \quad (1)$$

where  $\alpha_t$  is an increasing function of  $t$  and  $\sigma_t$  is a decreasing function of  $t$ . We expect that the model finds a marginal probability distribution  $p_t(x)$  that satisfies  $p_0(x) \equiv e(x)$  and  $p_1(x) \approx p(x)$ . We have the following Ordinary Differential Equation (ODE) to describe the velocity field:

$$\frac{dp_t(x)}{dt} + \nabla \cdot (p_t(x) \nu_\theta(x, t)) = 0 \quad (2)$$

where  $\nu_\theta(x, t)$  can be learned by minimizing the loss,

$$\mathcal{L}(\theta) = \mathbb{E}_{t \sim \mathcal{U}[0,1]} [ \| (x - \epsilon) - \nu_\theta(x, t) \|^2 ] \quad (3)$$

With learned  $\nu_\theta(x, t)$ , we can use the Monte Carlo method to approximate the integration. The inverse sampling of  $p_1(x)$  is generated by integrating the ODE from  $t = 0$  to  $t = 1$  by solving the discrete ODE by Euler method:

$$x_{t+1} = x_t + (\delta_{t+1} - \delta_t) \nu_\theta(x_t, t) \quad (4)$$

where  $\delta$  is the discrete timestep.

#### 3.2 Point cloud Upsampling via Flow Matching

We propose to leverage flow matching for point cloud upsampling. One related work is PUDM [Qu and et al., 2024], which learns a straightforward noise-to-data model, and then directly optimizes the  $l_2$  distance between the true and estimated point clouds. This approach has two limitations: 1) *sparse point clouds already contain partial views of the dense points, which encodes the underlying structure of the dense point clouds. Learning from noise is computationally costly and inefficient;* and 2) *Point clouds are unordered and have an irregular format, making it challenging for the model to pair points for learning tractable interpolation.* To resolve these issues, we propose a flow matching model PUFM for point cloud upsampling, which directly learns the optimal transport from sparse to dense distribution. To learn the flow matching model, we first densify the sparse point clouds and prealign them with the ground truth based on the Earth Mover’s Distance (EMD) [Chen and et al., 2020]. The overall framework is depicted in Figure 2.

**Point cloud flow matching.** Given the sparse point cloud  $x_0 \sim \mathcal{X}_{\text{sparse}} \in \mathbb{R}^{M \times 3}$  and dense point clouds  $x_1 \sim \mathcal{X}_{\text{dense}} \in \mathbb{R}^{N \times 3}$ . Our goal is to learn a flow matching model by finding the optimal transport between  $\mathcal{X}_{\text{sparse}}$  and  $\mathcal{X}_{\text{dense}}$ . Since the sparse point cloud is a partial view of dense point clouds but shares the same underlying 3D structure, we initially densify the sparse point cloud via a midpoint interpolation [He and et al., 2023] method. Given the sparse point clouds  $x_0$ , its

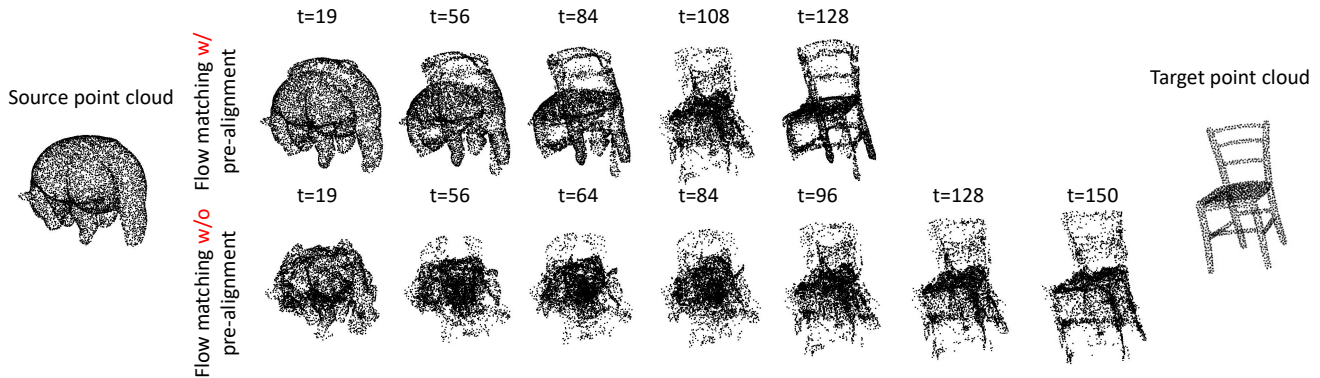


Figure 3: **A toy example on flow matching for point cloud transformation.** Without pre-alignment, the model converges slower as it first transforms the source point clouds to a set of dispersed clusters and then gradually matches to the target point clouds. In contrast, the pre-alignment exhibits more efficient and consistent transformation.

densified version  $\tilde{x}_0 = \text{mid}(x_0, \eta)$  can be defined as:

$$\tilde{x}_0 = \frac{1}{2} \cdot [\mathbf{R}_\gamma(x_0) + \text{FPS}(x_0, \gamma)] + \eta n, \quad \text{where } n \sim \mathcal{N}(0, I) \quad (5)$$

where  $\mathbf{R}_\gamma(\cdot)$  means repeating points by  $\gamma$  times and FPS denotes the Furthest Point Sampling [Yifan and et al., 2019]. Without losing generalization, we also add a small portion of Gaussian noise with noise level  $\eta$  to the sparse point cloud to simulate real-world noisy point clouds. The objective of learning a point cloud upsampling model can then be interpreted as learning the velocity field  $\nu$  from two distributions. We parameterize the velocity field by a network  $\nu_\theta(x_t, t)$  with learnable parameter  $\theta$ , and the loss term is defined as:

$$\mathcal{L}(\theta) = \min_{\theta} \mathbb{E}_{t, \tilde{x}_0, x_1} \|\nu_\theta(x_t, t) - [x_1 - \tilde{x}_0]\|^2, \quad (6)$$

where  $t \in [0, 1]$  and  $x_t$  are the timestep and the intermediate interpolant of the flow matching respectively.

**Point cloud pre-alignment.** In this work, we consider the upsampling follows a straight path [Lipman *et al.*, 2023] between sparse and dense distributions, *i.e.*:

$$x_t = (1 - t)\tilde{x}_0 + tx_1 \quad (7)$$

However, since the sparse point clouds are randomly sampled from their dense counterparts with additional noise, both  $\tilde{x}_0$  and  $x_1$  have an unordered format, which leads to a misalignment between the sparse and dense point clouds. The residual signal  $x_1 - \tilde{x}_0$  between two distributions varies significantly, leading to ambiguous learning by  $\nu_\theta(x_t, t)$ . To minimize Equation 6, the model finds it easier to spread the points uniformly across space. This causes a set of diffused ball-shaped clusters since the model will first solve these irregularities between these unpaired points by dispersing the points to a more tractable distribution, rather than approaching to the target distribution.

To illustrate this phenomenon, we conduct a toy experiment to learn a flow matching model that maps from the “bear” distribution to the “chair” distribution. As illustrated in Figure 3, the model without pre-alignment will disperse the points at the early stage, and the output is also blurry and

noisy. In contrast, the model with the pre-alignment demonstrates a consistent transformation from sparse to dense point clouds. It is worth noting that **the pre-alignment is applied only in the training phase**. Our model demonstrates higher efficiency as a result.

To this end, we propose to use the Earth Mover’s Distance (EMD) optimization [Chen and et al., 2020] to find an optimum assignment  $\phi^* = \phi(\tilde{x}_0, x_1)$  that minimizes the average distance for each point in the point cloud  $x_1$  to its nearest neighbor in  $x_0$ :

$$\phi^* = \underset{\phi}{\operatorname{argmin}} \Phi \sum_{i=1}^N \|x_1^{\phi(i)} - \tilde{x}_0^i\|_2, \quad (8)$$

where  $\Phi = 1, \dots, N \rightarrow 1, \dots, N$  is the set of possible bijective assignments between points in  $x_1$  and  $\tilde{x}_0$ . During the training stage, we first apply  $\phi^*$  to permute the dense point clouds, aligning them with the sparse point clouds. This alignment ensures that the model learns from a consistent pairing of sparse and dense point clouds. Next, we sample the interpolant  $x_t$  from the paired data. As shown in Figure 1, our approach demonstrates faster convergence when pre-alignment is applied, and high-fidelity dense point clouds can be generated in just a few sampling steps. In contrast, when pre-alignment is not applied, the model encounters early-stage collapse of the point clouds, hindering effective learning.

**Training and sampling** Based on our previous discussion, we now have the complete training scheme and sampling process. Furthermore, the distribution of  $t$  used during training has a clear impact on performance. We choose  $t = 1 - \cos(s\pi/2)$ ,  $s \sim \mathcal{U}[0, 1]$  to encourage the model to be certain of the direction to move at the very early steps of the procedure. A comparison of different sampling schemes can be found in the supplementary section. The complete training and sampling process is shown in Algorithm 1 and 2.

**Model architecture** We follow previous works [Luo and Hu, 2021; Qu and et al., 2024; Vogel and et al., 2024] and use a model architecture based on PointNet++ [Qi and et al., 2017]. It is a UNet structure that aggregates set abstraction (SA) and feature propagation (FP) blocks together to learn multi-scale point features. We add the vector attention blocks [Guo,

---

**Algorithm 1 Training**

---

**Require:**  $x_0 \sim \mathcal{X}_{sparse}, x_1 \sim \mathcal{X}_{dense}, t \sim \mathcal{U}[0, 1]$   
 $n \sim \mathcal{N}(0, I)$   
 $\tilde{x}_0 = \text{mid}(x_0, \eta)$   $\triangleright$  midpoint interpolation Eq 5  
 $\phi^* = \phi(\tilde{x}_0, x_1)$   $\triangleright$  EMD alignment Eq 8  
 $x_t \leftarrow (1-t)\tilde{x}_0 + tx_1^{\phi(i)}$   
 $l \leftarrow \|\nu_\theta(x_t, t) - (x_1^{\phi(i)} - \tilde{x}_0)\|^2$

---

---

**Algorithm 2 Sampling**

---

**Require:**  $x_0 \sim \mathcal{X}_{sparse}, \delta$   
 $x_t = \text{mid}(x_0, \eta)$   
**for**  $t = 0$  **to**  $1$  **do**  
     $x_{t+1} = (1 - \frac{\delta}{t})x_t + \frac{\delta}{t}\nu_\theta(x_t, t)$   
**end for**

---

2021; Wu and et al., 2022] at the last layer of SA blocks to encourage global feature mapping. The network is conditioned on the timestep  $t$  using sinusoidal positional embeddings. Both SA and FP blocks are included with conditional MLP layers that can incorporate the time embedding for feature extraction. The details of the model structure are shown in the supplementary.

## 4 Experiments

### 4.1 Experimental Details

**Dataset.** We use two public datasets for training and evaluation: PUGAN [Li *et al.*, 2019] and PU1K [Qian and et al., 2021]. We follow the same procedure in [Yifan and et al., 2019] to extract paired sparse and dense point clouds. Given the 3D meshes, we first use Poisson disk sampling to generate uniform patches as ground truth, each patch contains 1024 points. Then we randomly sample 256 points from each patch to obtain the sparse input data. For testing, we obtain 27 and 127 point clouds from PUGAN and PU1K, respectively. Code will be released soon.

**Evaluation metrics.** We use the Chamfer Distance (CD), Hausdorff Distance (HD) and Point-to-Surface (P2F) as the evaluations in our experiments.

### 4.2 Comparison with State-of-the-arts

We quantitatively evaluate our method with several point cloud upsampling approaches, including PUBP [Liu and et al., 2023], PUGCN [Qian and et al., 2021], PUGAN [Li *et al.*, 2019], PUDM [Qu and et al., 2024], Grad-PU [He and et al., 2023] and RepKPU [Rong and et al., 2024]. For fair comparison, we use the training parameters and model weights provided in the publicly available code bases for previous works. For the evaluation, we use randomly sampled sparse point clouds as input to compare different methods in  $4\times$  and  $16\times$  upsampling. In Table 1, we show the overall comparison to other state-of-the-art methods. We can see that ours achieves the best CD, HD and P2F scores, which indicates that ours delivers high-fidelity point clouds better than diffusion based models and other learning based approaches.

For visualization, Figure 4 shows the  $4\times$  upsampling results using different methods. To better visualize the point

Upscaling factors		$4\times$			$16\times$		
Dataset	Method	CD	HD	P2F	CD	HD	P2F
PUGAN	PUBP	1.649	1.476	5.997	0.982	2.071	7.496
	PUGCN	2.774	3.831	9.508	1.102	1.785	7.125
	RepKPU	1.067	1.139	1.974	0.384	1.245	2.151
	PUGAN	1.541	1.391	5.420	0.869	1.746	6.757
	PUDM	1.221	1.174	3.132	0.533	1.185	3.589
	Grad-PU	1.132	1.186	1.957	0.415	1.142	2.185
	<b>Ours</b>	<b>1.049</b>	<b>0.876</b>	<b>1.864</b>	<b>0.353</b>	<b>0.844</b>	<b>2.103</b>
PU1K	PUBP	0.694	0.593	2.206	0.343	0.712	2.958
	PUGCN	1.241	1.504	5.115	2.393	4.214	9.410
	RepKPU	0.566	0.619	1.464	0.290	0.592	<b>1.821</b>
	PUGAN	0.682	0.632	2.792	0.361	0.773	3.538
	PUDM	0.706	0.605	2.891	0.421	0.602	3.370
	Grad-PU	0.626	0.583	1.510	0.316	<b>0.552</b>	1.890
	<b>Ours</b>	<b>0.545</b>	<b>0.556</b>	<b>1.770</b>	<b>0.220</b>	0.578	1.983

Table 1: **Overall comparison on point cloud upsampling.** We report CD ( $10^{-4}$ ), HD ( $10^{-3}$ ) and P2F ( $10^{-3}$ ) on different methods. Ours outperforms baselines under different upsampling factors on different datasets.

Method	Grad-PU		PUDM		Ours	
	CD	HD	CD	HD	CD	HD
$5\times$	0.952	4.841	1.054	5.091	<b>0.921</b>	<b>4.763</b>
$7\times$	0.752	4.523	0.850	4.537	<b>0.708</b>	<b>4.363</b>
$8\times$	0.686	3.880	0.784	4.054	<b>0.638</b>	<b>3.947</b>
$12\times$	0.515	3.628	0.617	<b>3.371</b>	<b>0.455</b>	3.380
$20\times$	0.452	3.238	0.473	2.695	<b>0.344</b>	<b>2.666</b>
$24\times$	0.412	3.108	0.444	2.691	<b>0.314</b>	<b>2.690</b>
$32\times$	0.365	2.667	0.404	<b>2.322</b>	<b>0.273</b>	2.517

Table 2: **Arbitrary point clouds upsampling on PUGAN.** Ours can outperform baselines in CD and HD across different upsampling factors.

distributions, we highlight the parts in the red boxes, and we can see that ours can produce evenly distributed dense points, while others still produce noise or outlier points that do not follow the underlying surface. To further illustrate the upsampling quality, we apply the PCA normal estimation (neighborhood number = 15) [Hoppe and et al., 1992] and ball pivot approach (depth=9) [Bernardini and et al., 1999] to all upsampling point clouds for surface reconstruction. We can see that ours can produce smoother surfaces without showing any holes. For example, other approaches produce a hole in the leg of the elephant and noisy surfaces of the camel, while ours produces smooth results.

### 4.3 Arbitrary upsampling and denoising

Our proposed method can produce multi-scale point cloud upsampling as others [He and et al., 2023; Qu and et al., 2024] by repeatedly applying  $4\times$  upsampling and FPS downsampling. To show the versatility of ours, we compare ours with Grad-PU and PUDM on  $5\times$  to  $32\times$  upsampling and report the results in Table 2. We can see that ours steadily outper-

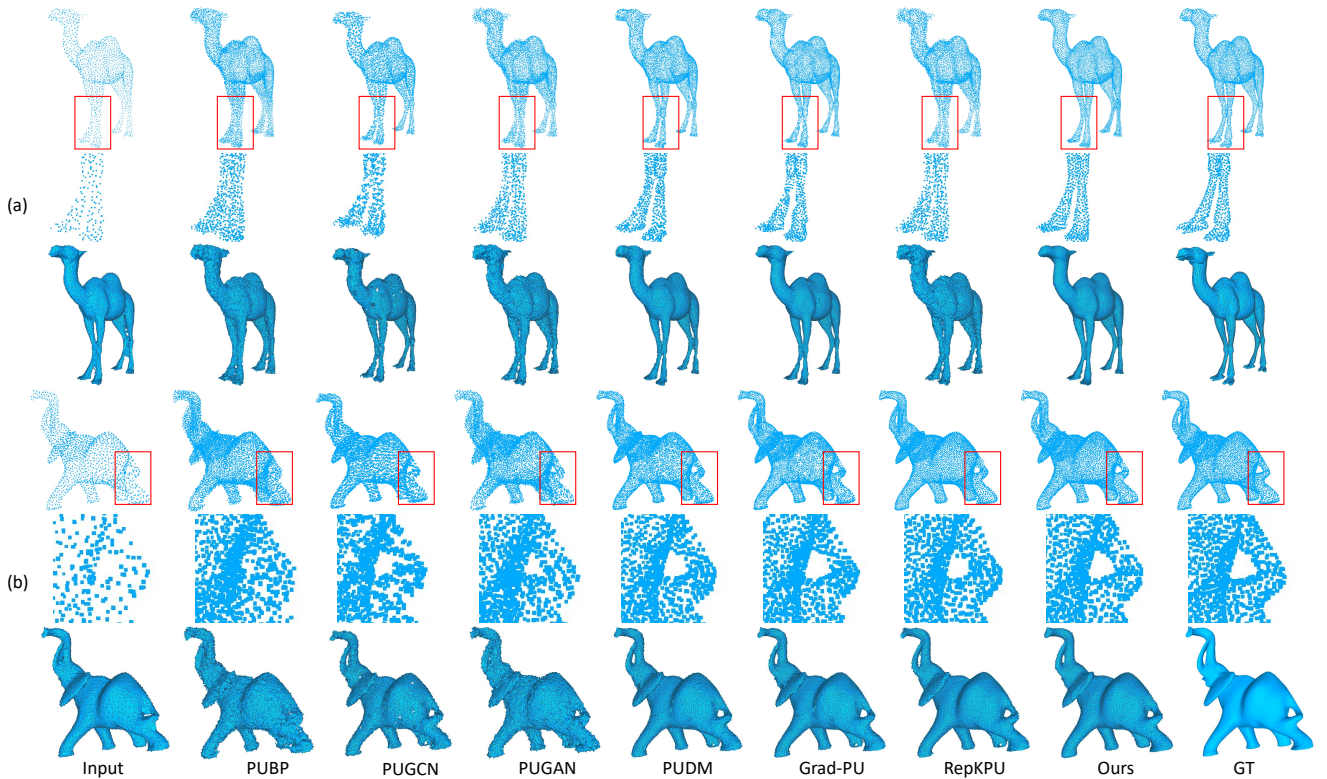


Figure 4: **Visual comparison of different methods on  $4\times$  upsampling.** We zoom in on the red box regions to highlight the point cloud upsampling differences. We also show the mesh reconstruction, and ours produces evenly distributed point clouds and smooth meshes.

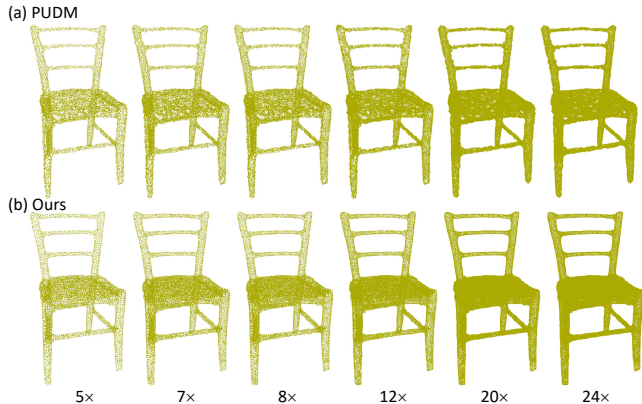


Figure 5: **Visualization of arbitrary point cloud upsampling.**

forms the other two methods in CD, HD, and P2F. We also show *Chair* example from PUGAN in Figure 5. We observe that PUDM produces holes on the surface of the chair, while ours can produce evenly distributed points without deviating from the underlying surface.

#### 4.4 Ablation Studies

As discussed in the previous section, ours is closely related to the diffusion model and inversion by direct iteration. To demonstrate the efficiency of our method, we compare with DDPM [Ho and et al., 2020], PUDM [Qu and et al., 2024]

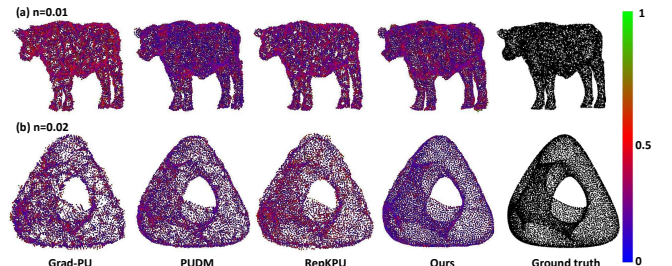


Figure 6: **Visualization of noisy point cloud upsampling.** We calculate the P2F distance as the color feature to the point cloud for visualization. Ours are visually better than baselines, without showing holes in (a) and noisy outliers in (b).

and InDI [Delbracio and Milanfar, 2023]. Note that DDPM and InDI were originally for image processing, and we modified them to achieve point-cloud upsampling. Table 3 shows that ours reduces the CD distance by approximately  $0.1\sim 0.2$  points and HD distance by approximately  $0.1\sim 0.2$  points. We also show the optimal sampling steps and the corresponding running time based on corresponding papers. We can see that ours uses the least sampling steps and achieves fast computation. This is due to the PC-to-PC flow matching which can reduce the restoration iterations. To demonstrate the impact of the proposed point cloud pre-alignment, we can see from row 4 and 5 that using proposed EMD pre-alignment is important for the flow matching model to start with reasonable

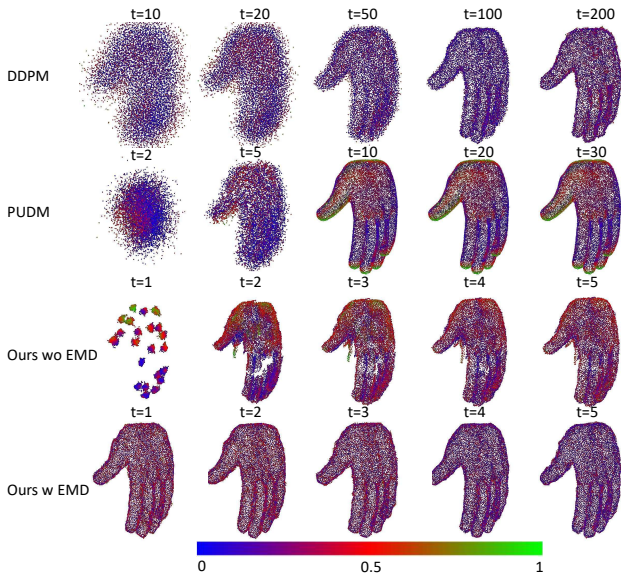


Figure 7: **Sample visualization at different time steps.** We compare with DDPM, PUDM, and ours at different sampling steps. Ours quickly learns the optimal upsampling point clouds, while others take longer sampling steps ( $> 10$ ).

Dataset	PUGAN			PU1K			Running time (s) sampling steps
	CD	HD	P2F	CD	HD	P2F	
DDPM	1.239	1.558	3.207	0.618	0.739	2.616	7.83/100
InDI	1.542	1.529	6.033	0.737	0.730	3.903	0.82/10
PUDM	1.221	1.174	3.132	0.706	0.605	2.891	1.83/30
Ours wo EMD	2.817	2.442	3.446	1.188	0.845	3.045	0.71/5
Ours w EMD	<b>1.049</b>	0.876	<b>1.864</b>	<b>0.545</b>	<b>0.556</b>	<b>1.770</b>	<b>0.71/5</b>

Table 3: **Ablation study on different inversion models.** We report the results on PUGAN and PU1K using different inversion models. The running time is calculated based on the optimal sampling steps reported in the corresponding papers.

point pairs for restoration. Without using the point cloud pre-alignment, the upsampling quality in all metrics drops significantly. This supports our discussion in Section 3.2 that the pre-alignment approximate the local region for point cloud upsampling, such that PUFM can model the distribution close to the ground truth.

Figure 7 shows the intermediate samples in different time steps. We represent the point clouds by encoding the P2F distances as RGB colors. We can see that ours can quickly converge to the ground truth point clouds with fewer errors (indicated by the blue color). We also observe that without using point cloud pre-alignment, the model first collapses into several clusters and then gradually reaches the ground truth data. Qualitative results, runtime, and experiments with other model setups are provided in the supplementary materials.

#### 4.5 Robustness and downstream applications

From Table 1, the most competitive methods are RepKPU, Grad-PU and PUDM. However, ours is more resilient to noise. To demonstrate the robustness of our method, we report the results in Table 4. Given the PUGAN dataset, we randomly add Gaussian noise with different levels ( $\eta$ ) to apply

Noise level	$\eta = 0.01$			$\eta = 0.02$		
	Method	CD	HD	P2F	CD	HD
PUDM	1.706	<b>1.803</b>	6.025	3.100	3.622	1.150
RepKPU	1.696	2.189	6.989	3.974	4.827	1.615
Grad-PU	1.795	1.965	6.591	3.588	4.248	1.310
Ours	<b>1.496</b>	1.879	<b>5.887</b>	<b>2.404</b>	<b>2.794</b>	<b>1.055</b>

Table 4:  **$4\times$  point cloud upsampling on noisy PUGAN.** Our performs better than others at different noise levels, indicating its robustness against noise.

$4\times$  upsampling. We can see that ours consistently performs better at different noise levels, with approximately 0.3~1.1 drops in terms of CD, HD and P2F. We are also interested in the upsampling performance on real-world data. We test ours and others on ScanNet [Dai *et al.*, 2017] and KITTI [Geiger and *et al.*, 2013] datasets. Without the ground truth data, we visualize the upsampled point clouds in Figure 8. We can see that ours performs better than PUDM in (a) of the bicyclist without showing gaps in the human body. In (b), ours can produce more evenly distributed dense points, revealing the indoor 3D layouts. We believe that directly using sparse point clouds as the prior for upsampling, ours remains consistent with real-world structures. The model does not need to hallucinate details entirely from Gaussian noise. More comparisons can be found in the supplementary.

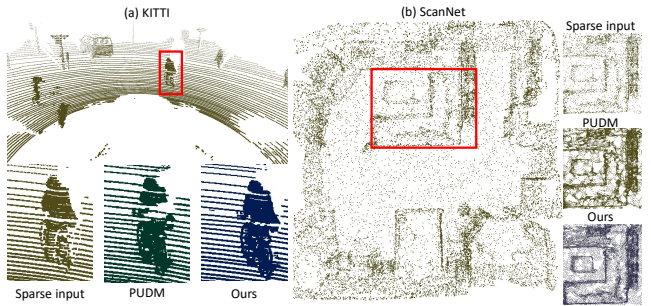


Figure 8: **Visualization of real point cloud upsampling.** We use two examples from ScanNet and KITTI to apply  $4\times$  upsampling. Compared to PUDM, ours does not show inconsistent patterns on the bicyclist or noisy point distribution in the living room.

## 5 Conclusion

In this paper, we introduce Point cloud Upsampling via Flow Matching (PUFM), an efficient framework that learns the direct optimal transport between sparse and dense point clouds. Unlike existing approaches that rely on direct  $l_2$  optimization, which often struggle with the unordered and irregular nature of point clouds, our method employs the optimization with EMD to pre-align sparse and dense point clouds before applying probability-based interpolation. Comprehensive experiments on both synthetic and real-world datasets demonstrate that PUFM consistently outperforms state-of-the-art methods in terms of accuracy and robustness. Additionally, PUFM achieves high efficiency compared to diffusion-based approaches and demonstrates strong resilience to noise and scalability across different input densities.

## References

- [Bernardini and et al., 1999] F. Bernardini and et al. The ball-pivoting algorithm for surface reconstruction. *IEEE Trans. Vis. Comput. Graph.*, 5(4):349–359, 1999.
- [Charles et al., 2017] R. Charles, H. Su, M. Kaichun, and L. J. Guibas. Pointnet: Deep learning on point sets for 3d classification and segmentation. In *IEEE Conf. Comput. Vis. Pattern Recog.*, pages 77–85, Los Alamitos, CA, USA, jul 2017.
- [Chen and et al., 2020] Yunlu Chen and et al. Pointmixup: Augmentation for point clouds. In *Eur. Conf. Comput. Vis.*, 2020.
- [Chen and et al., 2023] Haolan Chen and et al. Deep point set resampling via gradient fields. *IEEE Trans. Pattern Anal. Mach. Intell.*, 45(3):2913–2930, 2023.
- [Contributors, 2023] Pointcept Contributors. Pointcept: A codebase for point cloud perception research. <https://github.com/Pointcept/Pointcept>, 2023.
- [Dai et al., 2017] Angela Dai, Angel X. Chang, Manolis Savva, Maciej Halber, Thomas Funkhouser, and Matthias Nießner. Scannet: Richly-annotated 3d reconstructions of indoor scenes. In *Proc. Computer Vision and Pattern Recognition (CVPR), IEEE*, 2017.
- [Delbraccio and Milanfar, 2023] Mauricio Delbraccio and Peyman Milanfar. Inversion by direct iteration: An alternative to denoising diffusion for image restoration. 2023.
- [Feng and et al., 2022] Wanquan Feng and et al. Neural points: Point cloud representation with neural fields for arbitrary upsampling. In *IEEE Conf. Comput. Vis. Pattern Recog.*, 2022.
- [Geiger and et al., 2013] Andreas Geiger and et al. Vision meets robotics: The kitti dataset. *International Journal of Robotics Research (IJRR)*, 2013.
- [Guo, 2021] et al. Guo, MH. Pct: Point cloud transformer. *Comp. Visual Media*, (7):187–199, 2021.
- [Hanocka and et al., 2020] Rana Hanocka and et al. Point2mesh: A self-prior for deformable meshes. *ACM Trans. Graph.*, 39(4), 2020.
- [He and et al., 2023] Yun He and et al. Grad-pu: Arbitrary-scale point cloud upsampling via gradient descent with learned distance functions. In *IEEE Conf. Comput. Vis. Pattern Recog.*, pages 5354–5363, 2023.
- [Ho and et al., 2020] Jonathan Ho and et al. Denoising diffusion probabilistic models. In *Adv. Neural Inform. Process. Syst.*, 2020.
- [Hoppe and et al., 1992] Hugues Hoppe and et al. Surface reconstruction from unorganized points. In *Proceed. Computer Graphics and Interactive Techniques*, page 71–78, 1992.
- [Kerbl and et al., 2023] Bernhard Kerbl and et al. 3d gaussian splatting for real-time radiance field rendering. *ACM Trans. Graph.*, 42(4), July 2023.
- [Kumbar and et al., 2023] Akash Kumbar and et al. Tp-node: Topology-aware progressive noising and denoising of point clouds towards upsampling. In *Int. Conf. Comput. Vis.*, pages 2264–2274, 2023.
- [L. and et al., 2007] Yaron L. and et al. Parameterization-free projection for geometry reconstruction. In *ACM SIG-GRAPH*, page 22–es, New York, NY, USA, 2007.
- [Lemke and et al., 2024] Oliver Lemke and et al. Spot-compose: A framework for open-vocabulary object retrieval and drawer manipulation in point clouds. In *Int. Conf. on Robotics and Automation*, 2024.
- [Li and et al., 2021] Ruihui Li and et al. Point cloud upsampling via disentangled refinement. In *IEEE Conf. Comput. Vis. Pattern Recog.*, 2021.
- [Li et al., 2019] R. Li, X. Li, C. Fu, D. Cohen-Or, and P. Heng. Pu-gan: A point cloud upsampling adversarial network. *Int. Conf. Comput. Vis.*, pages 7202–7211, nov 2019.
- [Li et al., 2024] Jihe Li, Bo Pang, and Peng-Shuai Wang. Joint point cloud upsampling and cleaning with octree-based cnns. *arXiv preprint arXiv:2410.17001*, 2024.
- [Lipman and et al., 2023] Yaron Lipman and et al. Flow matching for generative modeling. In *The Eleventh International Conference on Learning Representations*, 2023.
- [Lipman et al., 2023] Yaron Lipman, Ricky TQ Chen, Heli Ben-Hamu, Maximilian Nickel, and Matt Le. Flow matching for generative modeling. In *Int. Conf. Learn. Represent.*, 2023.
- [Liu and et al., 2023] Zhi-Song Liu and et al. Arbitrary point cloud upsampling via dual back-projection network. In *IEEE Int. Conf. Image Process.*, pages 1470–1474, 2023.
- [Lu and et al., 2022] Xuequan Lu and et al. Low rank matrix approximation for 3d geometry filtering. *IEEE Trans. Vis. Comput. Graph.*, 28(4):1835–1847, 2022.
- [Luo and Hu, 2021] Shitong Luo and Wei Hu. Diffusion probabilistic models for 3d point cloud generation. In *IEEE Conf. Comput. Vis. Pattern Recog.*, June 2021.
- [Ma and et al., 2022] Xu Ma and et al. Rethinking network design and local geometry in point cloud: A simple residual mlp framework. *Int. Conf. Learn. Represent.*, 2022.
- [Mao et al., 2023] Aihua Mao, Zihui Du, Junhui Hou, Yaqi Duan, Yong-Jin Liu, and Ying He. Pu-flow: A point cloud upsampling network with normalizing flows. *IEEE Trans. Vis. Comput. Graph.*, 29(12):4964–4977, 2023.
- [Metzer and et al., 2021] Gal Metzer and et al. Self-sampling for neural point cloud consolidation. 40(5), 2021.
- [Park and et al., 2022] Chunghyun Park and et al. Fast point transformer. In *IEEE Conf. Comput. Vis. Pattern Recog.*, pages 16949–16958, June 2022.
- [Qi and et al., 2017] Charles R. Qi and et al. Pointnet++: deep hierarchical feature learning on point sets in a metric space. In *Adv. Neural Inform. Process. Syst.*, NIPS’17, page 5105–5114, 2017.



- [Qian and et al., 2020] Yue Qian and et al. Pugeo-net: A geometry-centric network for 3d point cloud upsampling. *arXiv*, abs/2002.10277, 2020.
- [Qian and et al., 2021] Guocheng Qian and et al. Pu-gcn: Point cloud upsampling using graph convolutional networks. In *IEEE Conf. Comput. Vis. Pattern Recog.*, pages 11683–11692, June 2021.
- [Qian and et al., 2024] Guocheng Qian and et al. Pointnext: revisiting pointnet++ with improved training and scaling strategies. In *Adv. Neural Inform. Process. Syst., NIPS '22*, 2024.
- [Qu and et al., 2024] Wentao Qu and et al. A conditional denoising diffusion probabilistic model for point cloud upsampling. In *IEEE Conf. Comput. Vis. Pattern Recog.*, pages 20786–20795, 2024.
- [Rong and et al., 2024] Yi Rong and et al. Repkpu: Point cloud upsampling with kernel point representation and deformation. In *IEEE Conf. Comput. Vis. Pattern Recog.*, pages 21050–21060, 2024.
- [Singh and et al., 2007] G. Singh and et al. Guest editors' introduction: Special section on acm vrst 2005. *IEEE Trans. Vis. Comput. Graph.*, 9(01):3–4, jan 2007.
- [Thomas and et al., 2019] Hugues Thomas and et al. Kpconv: Flexible and deformable convolution for point clouds. *Int. Conf. Comput. Vis.*, 2019.
- [Vaswani and et al., 2017] Ashish Vaswani and et al. Attention is all you need. In *Adv. Neural Inform. Process. Syst.*, volume 30, pages 5998–6008, 2017.
- [Vogel and et al., 2024] Mathias Vogel and et al. P2p-bridge: Diffusion bridges for 3d point cloud denoising. In *Eur. Conf. Comput. Vis.*, 2024.
- [Wang and et al., 2019] Yue Wang and et al. Dynamic graph cnn for learning on point clouds. *ACM Trans. Graph.*, 38(5), oct 2019.
- [Wenbo and et al., 2022] Zhao Wenbo and et al. Self-supervised arbitrary-scale point clouds upsampling via implicit neural representation. In *IEEE Conf. Comput. Vis. Pattern Recog.*, 2022.
- [Wu and et al., 2022] Xiaoyang Wu and et al. Point transformer v2: Grouped vector attention and partition-based pooling. In *Adv. Neural Inform. Process. Syst.*, 2022.
- [Wu and et al., 2024a] Xiaoyang Wu and et al. Point transformer v3: Simpler, faster, stronger. In *IEEE Conf. Comput. Vis. Pattern Recog.*, 2024.
- [Wu and et al., 2024b] Xiaoyang Wu and et al. Towards large-scale 3d representation learning with multi-dataset point prompt training. In *IEEE Conf. Comput. Vis. Pattern Recog.*, 2024.
- [Wu et al., 2022] Xiaoyang Wu, Yixing Lao, Li Jiang, Xihui Liu, and Hengshuang Zhao. Point transformer v2: Grouped vector attention and partition-based pooling. In *Adv. Neural Inform. Process. Syst.*, 2022.
- [Yang and et al., 2024] Zetong Yang and et al. Visual point cloud forecasting enables scalable autonomous driving. In *IEEE Conf. Comput. Vis. Pattern Recog.*, 2024.
- [Yifan and et al., 2019] W. Yifan and et al. Patch-based progressive 3d point set upsampling. *IEEE Conf. Comput. Vis. Pattern Recog.*, pages 5951–5960, jun 2019.
- [Yu and et al., 2018] L. Yu and et al. Pu-net: Point cloud upsampling network. *IEEE Conf. Comput. Vis. Pattern Recog.*, pages 2790–2799, jun 2018.
- [Yu and et al., 2021] Xumin Yu and et al. Pointtr: Diverse point cloud completion with geometry-aware transformers. In *Int. Conf. Comput. Vis.*, 2021.
- [Zhang and et al., 2019] Kuangen Zhang and et al. Linked dynamic graph cnn: Learning on point cloud via linking hierarchical features. *ArXiv*, abs/1904.10014, 2019.
- [Zhao et al., 2021] Hengshuang Zhao, Li Jiang, Jiaya Jia, Philip HS Torr, and Vladlen Koltun. Point transformer. In *Int. Conf. Comput. Vis.*, pages 16259–16268, 2021.